Original Article

Spirulina platensis and its ingredient biopterin glucoside improved insulin sensitivity in non-alcoholic steatohepatitis model

Yuri Fujihara,[1] Yasumasa Kodo,[2] Shin-ichi Miyoshi,[1] Ritsuko Watanabe,[3] Hiroshi Toyoda,[3] Mitsumasa Mankura,[4] Hideaki Kabuto,[5] and Fusako Takayama[1,*]

[1]Graduate School of Medicine, Dentistry and Pharmaceutical Sciences, Okayama University, 1-1-1 Tsushima-naka, Kita-ku, Okayama 700-8530, Japan
[2]Spirulina BioLab. Co., Ltd., 1-13-6 Nishinakajima, Yodogawa-ku, Osaka 532-0011, Japan
[3]Okayama Kyoritsu General Hospital, 8-10 Akasakahonmachi, Naka-ku, Okayama 703-8288, Japan
[4]Kurashiki Sakuyo University, 3515 Tamashima Nagao, Kurashiki, Okayama 710-0292, Japan
[5]Kagawa Prefectural College of Health Sciences, 281-1 Murechohara, Takamatsu, Kagawa 761-0123, Japan

(Received 15 December, 2020; Accepted 25 December, 2020; Published online 25 March, 2021)

Non-alcoholic steatohepatitis is the chronic liver disease leading to cirrhosis and cancer and its prevalence is increasing. Some agents are under clinical trials for non-alcoholic steatohepatitis treatment. We previously reported *Spirulina (Arthrospira) platensis* effectively prevented non-alcoholic steatohepatitis progression in our model rats. The contribution of phycocyanin, an ingredient of *Spirulina (Arthrospira) platensis*, was limited. We, therefore, have looked for more active components of *Spirulina (Arthrospira) platensis*. In this study, we pursued the effect of biopterin glucoside, another bioactive ingredient of *Spirulina (Arthrospira) platensis*. We found *Spirulina (Arthrospira) platensis* and biopterin glucoside oral administrations effectively alleviated oxidative stress, inflammation and insulin signal failure, and prevented fibroblast growth factor 21 gene overexpression in non-alcoholic steatohepatitis rat livers. We concluded biopterin glucoside is a major component of *Spirulina (Arthrospira) platensis* action.

***Key Words*: metabolic syndrome, oxidative stress, inflammation, insulin resistance**

Non-alcoholic steatohepatitis (NASH) is the hepatic manifestation of metabolic syndrome and an unfavourable chronic liver disease potentially leading to liver cirrhosis, hepatocellular carcinoma, and liver transplantation. The NASH global prevalence is estimated to be 3–5%. And mathematical modelling analyses indicated 15–56% increases of the NASH prevalence in 2030 compared to 2016.[1] In addition, the fact that some agents are now under the clinical trials for NASH treatment[2] indicates the necessity of NASH treatment and prevention. Because NASH onset and progression are closely related to the daily lifestyle, lifestyle modulation is recommended. The regular consumption of the functional food possessing the antioxidant or anti-inflammatory ability is also an approach for NASH management.

We previously revealed that the blue green algae *Spirulina (Arthrospira) platensis* (SP) prominently prevented the exacerbation of our NASH model.[3] We also investigated the effect of a SP ingredient phycocyanin but the contribution of phycocyanin to SP effect was limited.[3] This result suggested that other component(s) also contributed to the SP effect. Further pursuit of the active ingredient could improve SP utility and leads to find a new medical agent and supplement.

Biopterin glucoside (BPG) was isolated and identified from SP in 1999.[4] Because BPG is hydrolysed by α-glucosidase to give glucose and 2-amino-4-hydroxy-6-(1',2'-dihydroxypropyl) pteridine (biopterin),[5] oral administrated BPG is considered to be split by intestinal α-glucosidase and then absorbed as biopterin. Biopterin is completely oxidized form of tetrahydrobiopterin (BH4) and the biological activity of biopterin itself has not been reported. Although it was not clear how biopterin was converted to BH4 *in vivo*, it was reported that biopterin administration elevated BH4 level in mice body.[6] About BH4, it is the essential cofactor for aromatic amino acid hydroxylases[7–9] and endothelial nitric oxide synthase[10] and its deficiency disturbs folic acid metabolism involved with purine metabolism.[11] And further beneficial BH4 effects were reported. For examples, BH4 precursor sepiapterin supplementation decreased superoxide radicals in BH4 depleted endothelial cell mitochondria.[12] And BH4 administration lowered the fasting blood glucose level in streptozotocin (STZ)-induced diabetic model mice and obesity mice.[13] In spite of these beneficial effects, BH4 is easy to be oxidized[14] and its bioavailability is low. Specifically, 87% of the apparent renal BH4 elimination within 270 min took place in the first 120 min in rats[15] and the sum of BH4 and its oxidized form dihydrobiopterin (BH2) decreased in 2 h in rat liver, brain and kidney to the same level as before administration.[16] Moreover, the BH4 synthetic formulation sapropterin dihydrochloride used for hyperphenylalaninemia and phenylketonuria is the expensive agent because it is unstable against oxidation. For example, sapropterin dihydrochloride costs 68 kg body patient from $48,180 to 168,630 a year.[17] These facts suggest that using BH4 in other applications is difficult. In contrast to BH4, biopterin is more stable against oxidation than BH4 and gradually increases BH4 level in mice blood for 150 min after biopterin oral administration.[6] And the BH4 level was still higher in mice liver and kidney 3 h after biopterin oral administration than untreated.[6] Because of these biopterin advantages, revealing biopterin effects on health may contribute to the development of new agent which is easy to handle.

In this study, we pursued the mechanism of SP action on NASH progression and tried to make clear whether BPG contribute to the SP effect. Both oxidative stress and inflammation promote NASH progression. This crosstalk between oxidative stress and inflammation was stopped by SP in our previous study.[3] Inflammatory cytokines such as tumor necrosis factor-α (TNF-α) are triggers of insulin resistance.[18] Insulin

*To whom correspondence should be addressed.
E-mail: takayamf@cc.okayama-u.ac.jp

doi: 10.3164/jcbn.20-201

resistance aggravates the NASH state. Indeed, we previously observed insulin resistance in our NASH model rats by homeostasis model assessment-estimated insulin resistance (HOMA-IR) elevation (data not shown). And, it was reported that SP lowered the fasting blood glucose level in alloxan-induced diabetic model rats[19] and improved glucose tolerance in high-fat diet fed rats.[20] Although these reports suggested that SP affected the insulin signal pathway in NASH livers, such SP effects and which ingredient contributed to the SP effect have not been elucidated. Therefore, we investigated SP and BPG effects on oxidative stress, inflammation and insulin resistance in NASH model rats in this study.

Materials and Methods

Reagents. All chemicals we used in this study were guaranteed reagents except for particular descriptions.

Rats and housing. Six-week-old male Wistar rats, weighing 140–150 g, were purchased from SHIMIZU Laboratory Supplies Co., Ltd. (Kyoto, Japan). All rats were housed in the Animal Research Center of Okayama University under constant temperature (20–25°C) and humidity condition (40–50%) on a 12-h light/dark cycle (the dark cycle going from 8:00 pm until 8:00 am).

Animal study. In this study, SP and BPG effects on NASH were compared with the effect of insulin sensitizer pioglitazone (PGZ; Tokyo Chemical Industry Co., Ltd., Tokyo, Japan) as the standard agent. We had 8 groups; Control, choline-deficient high-fructose high-fat (CDHF), NASH, NASH + 2SP, NASH + 6SP, NASH + 4.6BPG, NASH + 13.7BPG, and NASH + 3PGZ. Rats were fed and treated as our previous study.[3] NASH + 2SP or NASH + 6SP group rats were 2 g/kg/day or 6 g/kg/day SP administrated. NASH + 4.6BPG or NASH + 13.7BPG group rats were 4.6 mg/kg/day or 13.7 mg/kg/day BPG, corresponding to the BPG amount included in 2 g/kg/day or 6 g/kg/day SP respectively, administrated. NASH + 3PGZ group rats were 3 mg/kg/day PGZ administrated. SP and BPG were offered by Spirulina Bio-Lab Co., Ltd. (Osaka, Japan). This animal experiment was based on the rules of Okayama University animal experiments and approved by the Animal Care and Use Committee, Okayama University (approval number: OKU-2018536). Every effort was performed to minimize the number of animals used and their distress.

Blood and liver tissue collection and preparation. At the end of the 10 weeks animal experiment, rats were sacrificed under anesthesia to collect blood and liver. Rat livers and plasma obtained from blood were kept at −80°C until sample preparation and proceeded for each analysis as previously described.[3]

Histopathological examination. Liver tissue was fixed with 10% formalin phosphate buffer, pH 7.4 was embedded in paraffin and sectioned at 4 μm thickness. After deparaffinization, sections were stained using Mayer's Hematoxylin Solution and Eosin.

Plasma assay for liver enzymes. Hepatobiliary injury was assessed by the activities of alanine aminotransferase (ALT), aspartate aminotransferase (AST) and alkaline phosphatase (ALP) in plasma. ALT and AST activities in plasma were measured by Transaminase CII-test Wako with the manufacturer's instructions. ALP activity was measured by Bessey, Lowry, and Brock method[21] with minor modifications.

Leukocyte priming status assessment. Reactive oxygen species (ROS) was detected by the chemiluminescence caused by the reaction with luminol after PMA stimulation as mentioned in the previous study[3] and used for the evaluation of leukocytes priming status.

Liver myeloperoxidase (MPO) activity assay. Liver MPO activity was measured by Schneider and Issekutz method[22] with minor modifications.

Protein quantifications by western blot analysis. Analysis of protein expression by western blot was performed by modifying our previous method.[3] Nuclear factor-κB (NF-κB) content in liver nuclei was assessed by using the primary antibody against NF-κB (sc-8008, mouse mAb; Santa Cruz Biotechnology, Dallas, TX). For insulin signal pathway, phospho-insulin receptor β, phospho-protein kinase B (Akt/PKB) and sterol regulatory element-binding protein-1c (SREBP-1c) expressions were quantified by using the primary antibodies against these proteins respectively; sc-81500 (mouse mAb; Santa Cruz Biotechnology, Inc.), #4060S (rabbit mAb; Cell Signaling Technology, Inc., Danvers, MA) and ab3259 (mouse mAb; Abcam plc., Cambridge, UK). As corresponding secondary antibody, goat anti-mouse IgG-HRP (sc-2031; Santa Cruz Biotechnology, Inc.) or goat anti-rabbit IgG H&L (HRP) (ab205718; Abcam plc.) was used. Generally, as housekeeping proteins, glyceraldehyde 3-phosphate dehydrogenase, β-actin, and Histone H1 are used. But, in our NASH model, these protein expressions were altered from control rat livers (data not shown) because of the change of nutrient energy metabolism, fibrosis, and oxidative stress. Therefore, we did not express housekeeping protein expressions. We made samples for western blot analysis with the same amount of total proteins with each other. Then, we loaded the same volume samples to equalize the loading dose.

Quantification of TNF-α. Plasma TNF-α level was quantified by Rat TNF-alpha Quantikine ELISA Kit (RTA00; R&D System, Minneapolis, MN) according to the manufacturer's instruction.

Fibroblast growth factor 21 (*Fgf21*) mRNA quantification by real time polymerase chain reaction (PCR). Total RNA in liver tissue was extracted from liver 25% homogenate using Quick Gene RNA tissue kit S II (Kurabo Industries Ltd., Osaka, Japan) as manufacture's instruction. Complementary DNA in liver tissue was synthesized from total RNA using High Capacity cDNA Reverse Transcription kits (4368814; Applied Biosystem, Thermo Fisher Scientific Inc., Waltham, MA) as manufacture's instruction. Then, real time PCR was performed using TaqMan Gene Expression Master Mix (4369016; Thermo Fisher Scientific Inc.) and Custom TaqMan Gene Expression Assay (4331348; Thermo Fisher Scientific Inc.) [*Fgf21* (Rn00590706) and an endogenous control 18S rRNA (4310893E)] as manufacture's instruction. The PCR condition was as follows; 2 min at 50°C, 10 min at 95°C, followed by 40 cycles of 15 s at 95°C for denaturing and 1 min at 60°C for annealing. Amplification data were analyzed by comparative Ct method and normalized to a housekeeping 18S rRNA gene expression.

Statistical analysis. Each quantitative result is expressed as the mean ± SEM. Statistical analysis was performed by one-way analysis of variance followed by Tukey's test using J-STAT. A value of $p<0.05$ was considered statistically significant.

Results

SP, BPG, and PGZ effects on NASH progression. Hepatobiliary enzyme activities in plasma reflect these enzymes leakage into blood. CDHF and NASH rats showed hepatic injury by hepatobiliary enzyme activities in plasma (Table 1). Histopathological views showed hepatosteatosis in CDHF and NASH rats. Moreover, inflammation, hepatocellular ballooning and severe fibrosis were also observed in NASH livers (Fig. 1). These changes consistent with the diagnostic criteria for NASH[23] were ameliorated by the oral administrations of SP, BPG, and PGZ (Fig. 1). The SP effect was the same as or larger than PGZ and reversed fatty liver.

Effects of SP, BPG, and PGZ on the oxidative stress and the inflammation in NASH livers. Luminol induced chemiluminescence reflects the amount of ROS by the primed peripheral leucocytes. The result showed that chemiluminescence

doi: 10.3164/jcbn.20-201

Table 1. Effects of SP, BPG, and PGZ on hepatobiliary damage with NASH progression

	ALT[§] (IU/L)	AST[‡] (IU/L)	ALP[†] (IU/L)
Control	16.2 ± 2.1	33.3 ± 4.8	212.4 ± 42.17
CDHF	18.9 ± 3.1	44.8 ± 1.0	717.0 ± 82.07##
NASH	25.5 ± 0.6#	57.0 ± 3.8#	831.9 ± 32.24##
NASH + 2SP	19.5 ± 0.7	37.0 ± 1.7*	195.0 ± 21.95**
NASH + 6SP	15.8 ± 0.5*	31.6 ± 2.9**	121.2 ± 18.39**
NASH + 4.6BPG	23.5 ± 0.8	41.4 ± 3.1*	385.8 ± 103.76**
NASH + 13.7BPG	20.0 ± 0.9	37.4 ± 2.6*	274.5 ± 64.75**
NASH + 3PGZ	19.2 ± 3.5	38.1 ± 0.8*	220.6 ± 51.86**

Liver index (%), liver wet weight/body weight ×100. Each value denotes the mean ± SEM of 5–7 rats. #$p<0.05$, ##$p<0.01$ vs control group, *$p<0.05$, **$p<0.01$ vs NASH group. [†]Alkaline phosphatase. [‡]Aspartate aminotransferase. [§]Alanine aminotransferase.

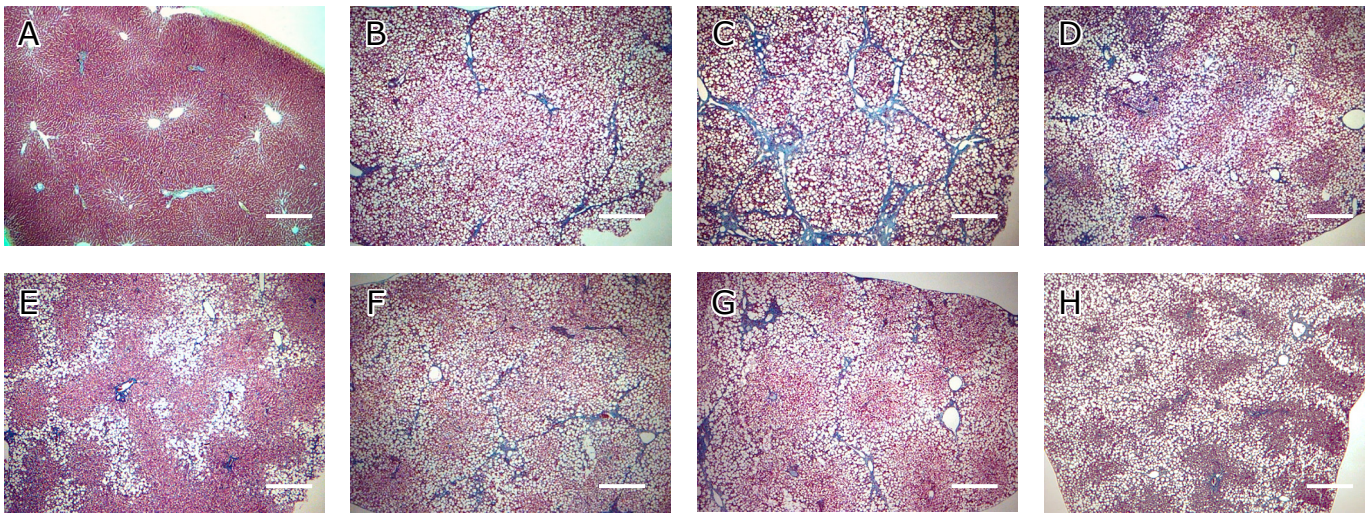

Fig. 1. SP, BPG, and PGZ effects on NASH progression. Histopathological views of experimental rat livers stained with masson trichrome. Scale bar = 200 μm. Following groups data were shown; (A) Control, (B) CDHF, (C) NASH, (D) NASH + 2SP, (E) NASH + 6SP, (F) NASH + 4.6BPG, (G) NASH + 13.7BPG, and (H) NASH + 3PGZ. See color figure in the on-line version.

from peripheral blood leukocytes increased in NASH by 4 fold compared to control (Fig. 2A). We determined the MPO activity to see the effective neutrophil infiltration to liver tissue. The MPO activity was elevated in CDHF and NASH livers by 5–6 fold compared to control (Fig. 2B). And SP, BPG, and PGZ administrations significantly ($p<0.05$) cancelled these changes in NASH rats (Fig. 2A and B). The NF-κB content in liver nuclei significantly ($p<0.01$) increased in NASH compared to control (Fig. 2C). The plasma TNF-α, one of the cytokines induced by NF-κB, increased in CDHF and NASH rat by 2–3 fold compared to control (Fig. 2D). And SP, BPG, and PGZ administrations significantly ($p<0.01$) decreased liver nuclear NF-κB and plasma TNF-α increases in NASH rats (Fig. 2C and D).

The liver insulin signal pathway alternation with NASH progression and SP, BPG, and PGZ effects on the insulin signal pathway in NASH livers. An inflammatory cytokine TNF-α is also a trigger of insulin resistance.[18] Actually, TNF-α was increased in NASH rat plasma (Fig. 2D). Therefore, we assessed the insulin signal activation in liver by the phosphorylated insulin receptor-β content. The phosphorylated insulin receptor-β significantly ($p<0.01$) increased in CDHF and NASH livers (Fig. 3A). Furthermore, we assessed Akt activation as the downstream of insulin signal by the phosphorylated Akt content in liver tissue. In spite of the phosphorylated insulin receptor-β increase, the phosphorylated Akt content decreased in CDHF and NASH livers to about half level of control (Fig. 3B). These changes indicated the insulin signal failure between insulin receptor and Akt in NASH livers, which was recalled by SP, BPG, and PGZ administrations (Fig. 3A and B). Then, SREBP-1c, the lipogenetic transcription factor partly regulated by insulin, expression was assessed. SREBP-1c expression significantly ($p<0.01$) increased in NASH livers. And SP, BPG, and PGZ administrations significantly ($p<0.01$) decreased SREBP-1c expression increase in NASH livers (Fig. 3C). In relation to the discrepancy between the phosphorylated insulin receptor-β and the phosphorylated Akt content alternations in NASH livers, we investigated the endocrine factor FGF21 which is reported to improve insulin sensitivity through Akt activation.[24] Real time PCR assay exhibited the *Fgf21* mRNA expression increases in CDHF and NASH livers by 60–100 fold compared to Control. And SP, BPG, and PGZ administrations significantly ($p<0.05$) decreased the increase of the *Fgf21* mRNA expression in NASH livers (Fig. 3D).

Discussion

In our previous study, we showed that SP effectively prevented NASH progression and improved fatty liver. However, a SP ingredient phycocyanin did not fully cover the SP effect.[3] Therefore, we pursued the active ingredient of SP in the present

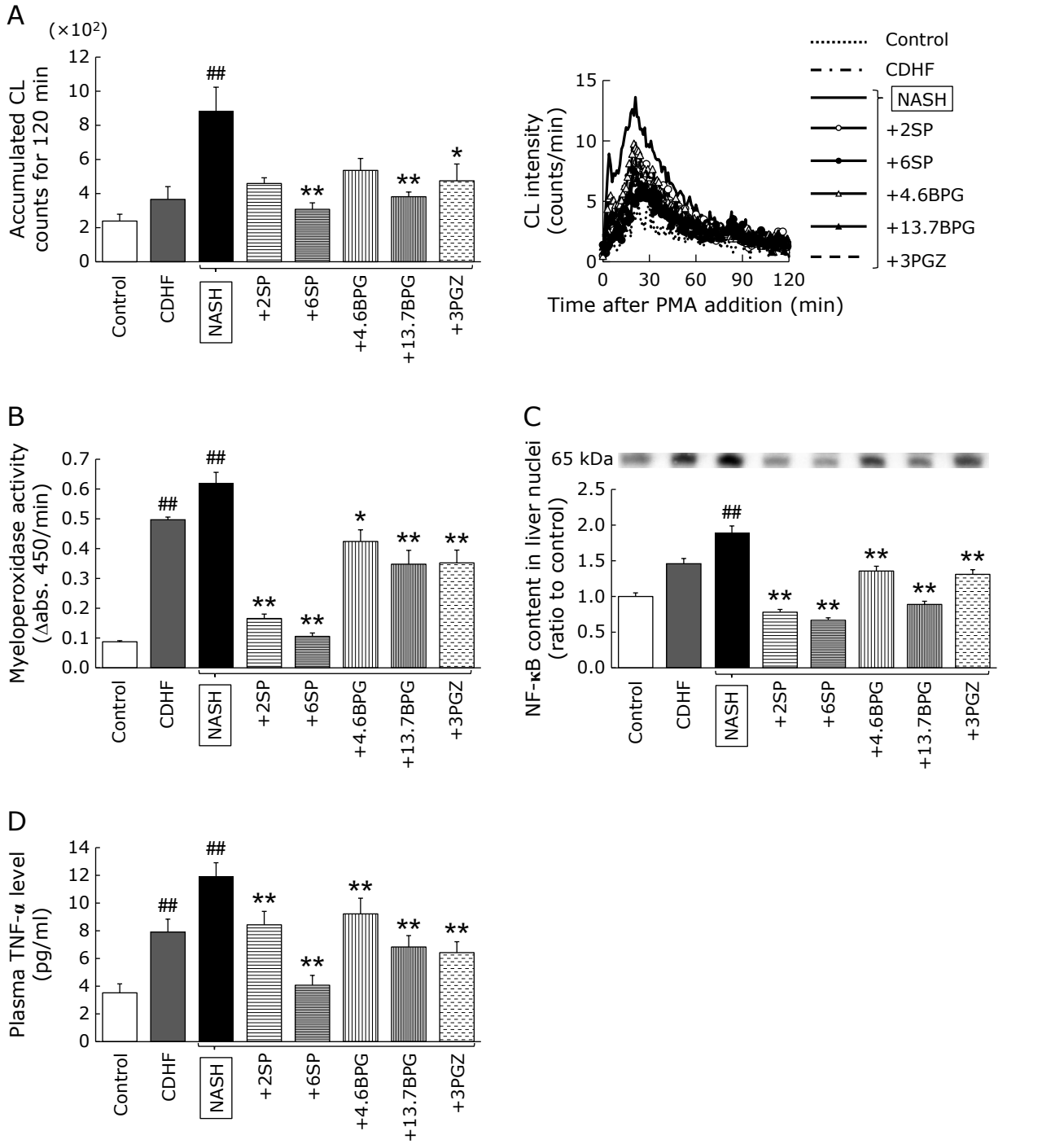

Fig. 2. Effects of SP, BPG, and PGZ on the oxidative stress and inflammation. (A) Reactive oxygen species (ROS) generated by primed leukocytes. Accumulated chemiluminescence (CL) intensity for 120 min was expressed. (B) Myeloperoxidase (MPO) activity in liver tissue. The variation of absorbance per minute was expressed as MPO activity. (C) Nuclear factor-kappa B (NF-κB) activation in liver indicated by its content in liver nuclei. Sample apply amounts, 22.5 μg protein/15 μl. (D) Plasma TNF-α level. Each value denotes the mean ± SEM of 5–7 rats. $^{\#\#}p<0.01$ vs control group, $^{*}p<0.05$, $^{**}p<0.01$ vs NASH group.

study. In this study, we assessed the SP and its ingredient BPG effects on our NASH model rats by comparing with the insulin sensitizer PGZ. In this paper, we report that SP and BPG prevented NASH progression. Whole SP improved fatty liver and the effect was greater than PGZ.

In our previous study, SP interfered with the link between oxidative stress and inflammation in NASH rats. An inflammatory cytokine TNF-α causes insulin resistance[18] which is the major factor of NASH progression. Additionally, there was the HOMA-IR elevation in NASH model in our previous study (data not shown). Therefore, we focused on the insulin signal pathway in NASH livers in this study. And we assessed SP and BPG effects on the oxidative stress, the inflammation, and the insulin signal pathway in NASH rats.

doi: 10.3164/jcbn.20-201

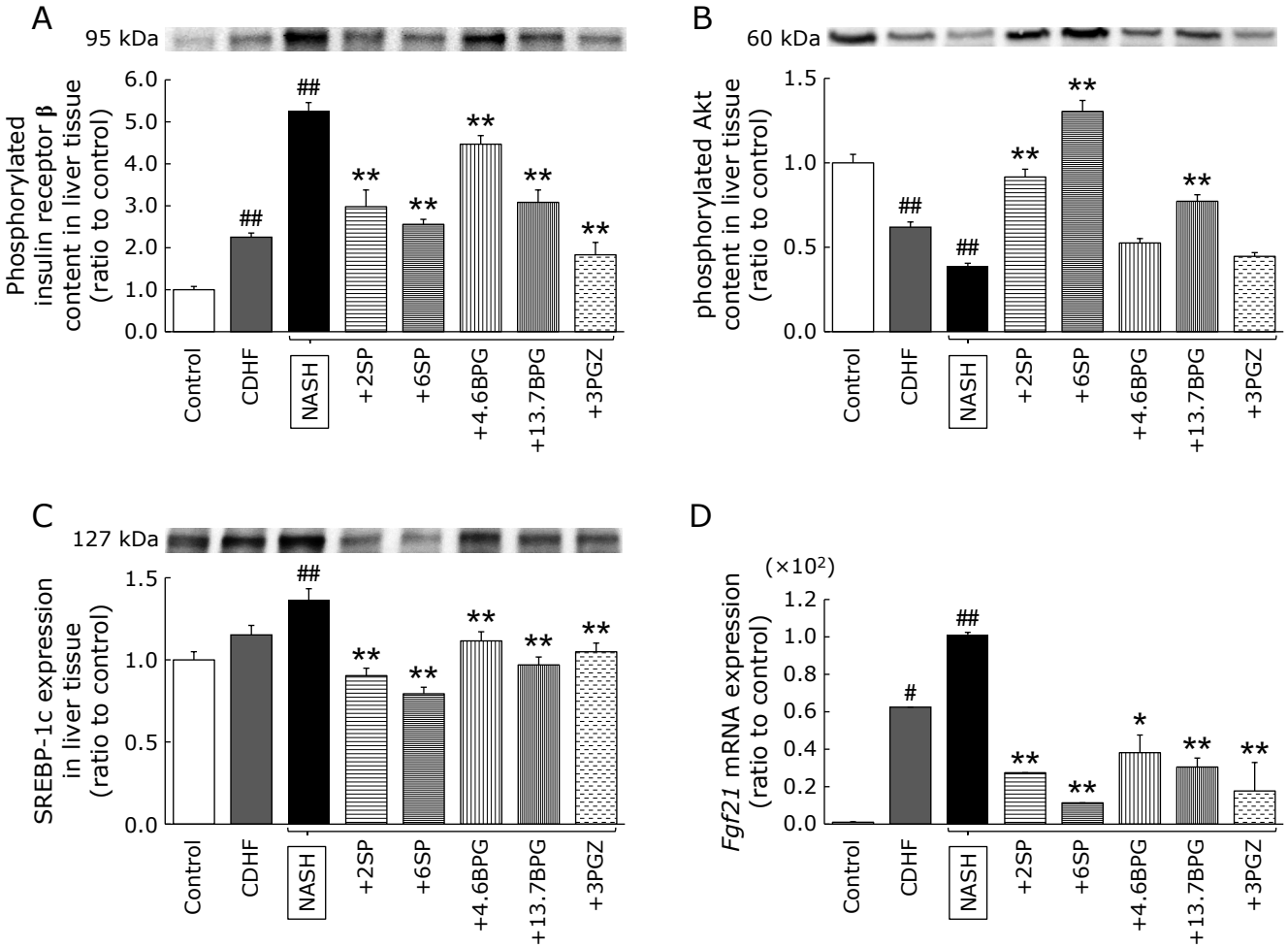

Fig. 3. Effects of SP, BPG, and PGZ on insulin signal pathway. (A, B, C) Sample apply amounts, 30 μg protein/10 μl. (A) Insulin receptor-β activation with phosphorylation in liver tissue. (B) Protein kinase B (Akt/PKB) activation with phosphorylation in liver tissue. (C) Sterol regulatory element-binding protein-1c (SREBP-1c) expression in liver tissue. (D) Fibrosis growth factor 21 (*Fgf21*) mRNA expression was normalized to 18S rRNA level. The control group value was expressed as 1. Each value denotes the mean ± SEM of 5–7 rats. $^{\#}p<0.05$, $^{\#\#}p<0.01$ vs control group, $^{*}p<0.05$, $^{**}p<0.01$ vs NASH group.

The oxidative stress and the inflammation are closely related with each other. For example, sustained ROS generation by leukocytes is a factor of the chronic inflammation.[25] Indeed, in this study, ROS generation by peripheral blood leukocytes with priming and neutrophil infiltration into liver tissue were enhanced in NASH rats, which were mitigated by SP and BPG administrations. Moreover, the oxidative stress and the inflammation were linked by NF-κB with a loop. Specifically, various stimulations such as ROS and inflammatory cytokines including TNF-α activate NF-κB.[26] Then, activated NF-κB upregulates cytokines such as TNF-α and ROS generating enzymes.[27] In the present study, to assess the crosstalk between the oxidative stress and the inflammation, we analysed NF-κB activation. In NASH livers, NF-κB activation was promoted and formed the link between the oxidative stress and the inflammation, which was broken off by SP and BPG administrations. TNF-α is one of the most abundant mediators in inflamed tissue. TNF-α enhances inflammation through inflammatory cytokine induction[28] and also causes insulin resistance.[18]

Because of the plasma TNF-α level elevation in NASH rats, we investigated the insulin signal pathway in NASH livers and SP and BPG effects. Although the increase in phosphorylated insulin receptor-β content indicates the excessive insulin signal activation in NASH livers, its downstream activation by Akt phosphorylation was impaired in NASH livers. These results demonstrated the signal failure between insulin receptor and Akt in NASH livers. Normally, insulin prevents glucogenesis through PI3K/Akt/FOXO1 pathway.[29] Therefore, impaired Akt activation showed in this study may have promoted glucogenesis followed by the blood glucose elevation in NASH rats.[30] Glucose is used for the energy generation and surplus glucose is restored as glycogen. And glucose beyond the glycogen storage capacity is used as the substrate of fatty acid synthesis.[31] SREBP-1c is also induced by insulin stimulation[32] and plays a vital role in fatty acid and triglyceride synthesis through regulating lipogenetic genes.[33] The increased glucose on NASH rats[30] provided more acetyl CoA, a substrate of lipogenesis, by glycolysis. Then, lipogenetic regulator SREBP-1c expression increased in CDHF and NASH livers, contrary to decreased phosphorylated Akt. This dissociation of insulin signal downstream alternations in NASH livers suggested the "selective insulin resistance". Excessive insulin stimulation causes unquenchable fatty acid generation, which damages the insulin signal and cause further selective insulin resistance.[34] In this study, SP and BPG impaired excessive insulin signal activation,

promoted Akt activation, and decreased SREBP-1c expression in NASH livers. By these results, we assumed that SP and BPG cancelled selective insulin resistance and reversed steatosis in NASH livers. Except insulin signal, lipid metabolism is regulated by many factors such as AMP-activated protein kinase α.[35] Therefore, further investigation about other pathways is required for pursuing the mechanism of SP and BPG effects on lipid metabolism in future.

In relation to the selective insulin resistance, we focused on FGF21. FGF21 is an endocrine factor induced by glucose[36] and fructose.[37] It was reported that FGF21 improved insulin sensitivity through Akt activation in rat livers fed with high-fat high-sucrose diets[24] and downregulated lipogenetic genes in high-fat diets-induced obesity mice.[38] Excessive fructose intake by CDHF diets and the blood glucose level elevation[30] caused by insulin receptor-Akt signal failure induced *Fgf21* mRNA expression in NASH livers. It was reported that lipogenetic regulation by FGF21 was impaired by free fatty acid in HepG2 cells.[39] In this study, selective insulin resistance causing excessive fatty acid synthesis may have impaired FGF21 effect, which lead to the further insulin resistance. Selective insulin resistance may make a loop with the failure of FGF21 effect. SP and BPG administrations may have reduced *Fgf21* mRNA inducer glucose through Akt activation in NASH livers. Therefore, *Fgf21* mRNA expression decreased in SP and BPG administrated rat livers to less than half level of NASH. It was possible that less *Fgf21* mRNA was sufficient to regulate insulin sensitivity and lipogenesis because SP and BPG administrations improved fatty lives. It was suggested that SP and BPG broke off the loop between selective insulin resistance and the failure of FGF21 effect.

In this paper, we showed SP and BPG ameliorated NASH by interfering with insulin signal pathway, oxidative stress, and inflammation. BPG is thought to be hydrolysed by α-glucosidase[5] and absorbed as biopterin in intestine. Absorbed biopterin in this study may have exerted the effect through the conversion to BH4 by unrevealed pathway.[6] It was reported that exogenous BH4 supplementation was inefficient to elevate cellular BH4 level compared to another BH4 precursor sepiapterin.[40] *In vivo*, sepiapterin more efficiently elevated BH4 level than supplemented BH4 itself in liver, kidney, and blood.[41] The reason may be that exogenous BH4 is needed to be oxidized to BH2 to pass across plasma membranes because BH4 itself is hydrophilic,[40] and BH2 is then reduced back to BH4 by dihydrofolate reductase. Indeed, the small BH4 level elevation in liver and kidney by BH4 supplementation was disturbed by methotrexate, a dihydrofolate reductase inhibitor.[41] These reports suggest that BH4 precursors contribute for the maintenance of BH4 level in the body. Taking these consideration into account, there may be the efficient pathway converting from BPG of SP to BH4 to work efficiently to prevent our NASH model.

Acknowledgments

This work was supported by the Japan Society for the Promotion of Science, Grant number 25350886. We would like to express the appreciation to Shigeru Okada (Graduate School of Medicine, Dentistry and Pharmaceutical Sciences, Okayama University, Okayama, Japan) for revision of this manuscript.

Abbreviations

Akt/PKB	protein kinase B
ALP	alkaline phosphatase
ALT	alanine aminotransferase
AST	aspartate aminotransferase
BH2	dihydrobiopterin
BH4	tetrahydrobiopterin
BPG	biopterin glucoside
CDHF	choline-deficient high-fructose high-fat
FGF21	fibrosis growth factor 21
HOMA-IR	homeostasis model assessment-estimated insulin resistance
MPO	myeloperoxidase
NASH	non-alcoholic steatohepatitis
NF-κB	nuclear factor-κB
PCR	polymerase chain reaction
PGZ	pioglitazone
ROS	reactive oxygen species
SP	*Spirulina (Arthrospira) platensis*
SREBP-1c	sterol regulatory element-binding protein-1c
TNF-α	tumor necrosis factor-α

Conflict of Interest

No potential conflicts of interest were disclosed.

References

1 Estes C, Anstee QM, Arias-Loste MT, *et al*. Modeling NAFLD disease burden in China, France, Germany, Italy, Japan, Spain, United Kingdom, and United States for the period 2016–2030. *J Hepatol* 2018; **69**: 896–904.
2 Connolly JJ, Ooka K, Lim JK. Future pharmacotherapy for non-alcoholic steatohepatitis (NASH): review of phase 2 and 3 trials. *J Clin Transl Hepatol* 2018; **6**: 264–275.
3 Pak W, Takayama F, Mine M, *et al*. Anti-oxidative and anti-inflammatory effects of spirulina on rat model of non-alcoholic steatohepatitis. *J Clin Biochem Nutr* 2012; **51**: 227–234.
4 Noguchi Y, Ishii A, Matsushima A, *et al*. Isolation of biopterin-alpha-glucoside from *Spirulina (Arthrospira) platensis* and its physiologic function. *Mar Biotechnol (NY)* 1999; **1**: 207–210.
5 Forrest HS, Van Baalen C, Myers J. Isolation and identification of a new pteridine from a blue-green alga. *Arch Biochem Biophys* 1958; **78**: 95–99.
6 Hasegawa H, Sawabe K, Shimizu I, *et al*. Composition containing biopterin and method for using the same. WIPO IP Portal. https://patentscope2.wipo.int/search/en/detail.jsf?docId=WO2007119367&tab=PCTBIBLIO. Accessed January 13, 2021
7 Kaufman S. The structure of the phenylalanine-hydroxylation cofactor. *Proc Natl Acad Sci U S A* 1963; **50**: 1085–1093.
8 Nagatsu T, Levitt M, Udenfriend S. Tyrosine hydroxylase. The initial step in norepinephrine biosynthesis. *J Biol Chem* 1964; **239**: 2910–2917.
9 Lovenberg W, Jequier E, Sjoerdsma A. Tryptophan hydroxylation: measurement in pineal gland, brainstem, and carcinoid tumor. *Science* 1967; **155**: 217–219.
10 Kwon NS, Nathan CF, Stuehr DJ. Reduced biopterin as a cofactor in the generation of nitrogen oxides by murine macrophages. *J Biol Chem* 1989; **264**: 20496–20501.
11 Xu F, Sudo Y, Sanechika S, *et al*. Disturbed biopterin and folate metabolism in the Qdpr-deficient mouse. *FEBS Lett* 2014; **588**: 3924–3931.
12 Bailey J, Shaw A, Fischer R, *et al*. A novel role for endothelial tetrahydrobiopterin in mitochondrial redox balance. *Free Radic Biol Med* 2017; **104**: 214–225.
13 Abudukadier A, Fujita Y, Obara A, *et al*. Tetrahydrobiopterin has a glucose-lowering effect by suppressing hepatic gluconeogenesis in an endothelial nitric oxide synthase-dependent manner in diabetic mice. *Diabetes* 2013; **62**: 3033–3043.
14 Alkaitis MS, Crabtree MJ. Recoupling the cardiac nitric oxide synthases: tetrahydrobiopterin synthesis and recycling. *Curr Heart Fail Rep* 2012; **9**: 200–210.
15 Ohashi A, Saeki Y, Harada T, *et al*. Tetrahydrobiopterin supplementation: elevation of tissue biopterin levels accompanied by a relative increase in

doi: 10.3164/jcbn.20-201

dihydrobiopterin in the blood and the role of probenecid-sensitive uptake in scavenging dihydrobiopterin in the liver and kidney of rats. *PLoS One* 2016; **11**: e0164305.
16 Ohashi A, Suetake Y, Saeki Y, Harada T, Aizawa S, Hasegawa H. Rapid clearance of supplemented tetrahydrobiopterin is driven by high-capacity transporters in the kidney. *Mol Genet Metab* 2012; **105**: 575–581.
17 Pharmacoeconomic Review Report: Sapropterin dihydrochloride (Kuvan) [Internet]. In: *CADTH Common Drug Reviews*, Ottawa: Canadian Agency for Drugs and Technologies in Health, 2017; 9–10.
18 Akash MSH, Rehman K, Liaqat A. Tumor necrosis factor-alpha: role in development of insulin resistance and pathogenesis of type 2 diabetes mellitus. *J Cell Biochem* 2018; **119**: 105–110.
19 Aissaoui O, Amiali M, Bouzid N, Belkacemi K, Bitam A. Effect of *Spirulina platensis* ingestion on the abnormal biochemical and oxidative stress parameters in the pancreas and liver of alloxan-induced diabetic rats. *Pharm Biol* 2017; **55**: 1304–1312.
20 Vidé J, Bonafos B, Fouret G, *et al*. *Spirulina platensis* and silicon-enriched spirulina equally improve glucose tolerance and decrease the enzymatic activity of hepatic NADPH oxidase in obesogenic diet-fed rats. *Food Funct* 2018; **9**: 6165–6178.
21 Bessey OA, Lowry OH, Brock MJ. A method for the rapid determination of alkaline phosphates with five cubic millimeters of serum. *J Biol Chem* 1946; **164**: 321–329.
22 Schneider T, Issekutz AC. Quantitation of eosinophil and neutrophil infiltration into rat lung by specific assays for eosinophil peroxidase and myeloperoxidase. Application in a Brown Norway rat model of allergic pulmonary inflammation. *J Immunol Methods* 1996; **198**: 1–14.
23 Kleiner DE, Brunt EM, Van Natta M, *et al*.; Nonalcoholic Steatohepatitis Clinical Research Network. Design and validation of a histological scoring system for nonalcoholic fatty liver disease. *Hepatology* 2005; **41**: 1313–1321.
24 Gong Q, Hu Z, Zhang F, *et al*. Fibroblast growth factor 21 improves hepatic insulin sensitivity by inhibiting mammalian target of rapamycin complex 1 in mice. *Hepatology* 2016; **64**: 425–438.
25 Kruger P, Saffarzadeh M, Weber AN, *et al*. Neutrophils: between host defence, immune modulation, and tissue injury. *PLoS Pathog* 2015; **11**: e1004651.
26 Lorenzo O, Picatoste B, Ares-Carrasco S, Ramírez E, Egido J, Tuñón J. Potential role of nuclear factor κB in diabetic cardiomyopathy. *Mediators Inflamm* 2011; **2011**: 652097.
27 Morgan MJ, Liu ZG. Crosstalk of reactive oxygen species and NF-κB signaling. *Cell Res* 2011; **21**: 103–115.
28 Maini RN, Elliott MJ, Brennan FM, Feldmann M. Beneficial effects of tumour necrosis factor-alpha (TNF-alpha) blockade in rheumatoid arthritis (RA). *Clin Exp Immunol* 1995; **101**: 207–212.
29 Semple RK, Sleigh A, Murgatroyd PR, *et al*. Postreceptor insulin resistance contributes to human dyslipidemia and hepatic steatosis. *J Clin Invest* 2009; **119**: 315–322.
30 Takayama F, Egashira T, Kawasaki H, *et al*. A novel animal model of nonalcoholic steatohepatitis (NASH): hypoxemia enhances the development of NASH. *J Clin Biochem Nutr* 2009; **45**: 335–340.
31 Adeva-Andany MM, Pérez-Felpete N, Fernández-Fernández C, Donapetry-García C, Pazos-García C. Liver glucose metabolism in humans. *Biosci Rep* 2016; **36**: e00416.
32 Hegarty BD, Bobard A, Hainault I, Ferré P, Bossard P, Foufelle F. Distinct roles of insulin and liver X receptor in the induction and cleavage of sterol regulatory element-binding protein-1c. *Proc Natl Acad Sci U S A* 2005; **102**: 791–796.
33 Shimano H. SREBPs: physiology and pathophysiology of the SREBP family. *FEBS J* 2009; **276**: 616–621.
34 Brown MS, Goldstein JL. Selective versus total insulin resistance: a pathogenic paradox. *Cell Metab* 2008; **7**: 95–96.
35 Ashida H, Tian X, Kitakaze T, Yamashita Y. Bisacurone suppresses hepatic lipid accumulation through inhibiting lipogenesis and promoting lipolysis. *J Clin Biochem Nutr* 2020; **67**: 43–52.
36 Iizuka K, Takeda J, Horikawa Y. Glucose induces FGF21 mRNA expression through ChREBP activation in rat hepatocytes. *FEBS Lett* 2009; **583**: 2882–2886.
37 Fisher FM, Kim M, Doridot L, *et al*. A critical role for ChREBP-mediated FGF21 secretion in hepatic fructose metabolism. *Mol Metab* 2016; **6**: 14–21.
38 Xu J, Lloyd DJ, Hale C, *et al*. Fibroblast growth factor 21 reverses hepatic steatosis, increases energy expenditure, and improves insulin sensitivity in diet-induced obese mice. *Diabetes* 2009; **58**: 250–259.
39 Asrih M, Montessuit C, Philippe J, Jornayvaz FR. Free fatty acids impair FGF21 action in HepG2 cells. *Cell Physiol Biochem* 2015; **37**: 1767–1778.
40 Hasegawa H, Sawabe K, Nakanishi N, Wakasugi OK. Delivery of exogenous tetrahydrobiopterin (BH4) to cells of target organs: role of salvage pathway and uptake of its precursor in effective elevation of tissue BH4. *Mol Genet Metab* 2005; **86** Suppl 1: S2–S10.
41 Sawabe K, Wakasugi KO, Hasegawa H. Tetrahydrobiopterin uptake in supplemental administration: elevation of tissue tetrahydrobiopterin in mice following uptake of the exogenously oxidized product 7,8-dihydrobiopterin and subsequent reduction by an anti-folate-sensitive process. *J Pharmacol Sci* 2004; **96**: 124–133.